EUROPEAN FUSION DEVELOPMENT AGREEMENT
JET

EFDA–JET–PR(02)10

O. Barana et al

Real-Time Determination of Internal Inductance and Magnetic Axis Radial Position in JET

Real-Time Determination of Internal Inductance and Magnetic Axis Radial Position in JET

O. Barana[1], A. Murari[1], E. Joffrin[2], F. Sartori[3]
and contributors to the EFDA-JET workprogramme*

[1]Consorzio RFX - Associazione EURATOM/ENEA sulla Fusione, Corso Stati Uniti 4, 35127 Padova, Italy.
[2]Association EURATOM/CEA, CEA Cadarache, Bâtiment 513, F-13108 Saint-Paul-lez-Durance, France.
[3]EURATOM/UKAEA Fusion Association, Culham Science Centre, Abingdon, Oxon OX14 3DB, UK.
** See annex of J. Pamela et al, "Overview of Recent JET Results and Future Perspectives", Fusion Energy 2000 (Proc. 18th Int. Conf. Sorrento, 2000), IAEA, Vienna (2001).*

Paper to be submitted for publication in PPCF

ABSTRACT
The internal inductance l_i and the magnetic axis radial position R_{MAG} are important elements in the development of a reliable real-time control system.

Specific algorithms have been developed to obtain these quantities and, with the aim of comparing the relative performances, l_i and R_{MAG} have also been determined with suitable Neural Networks. Both procedures rely on the Shafranov Integrals, which have been computed on the plasma Last Closed Flux Surface using an updated version of the fast boundary code XLOC.

The two approaches have been verified on several classes of equilibrium and both in the limiter and x-point phases of the discharges. Their results have been measured against the estimates of the off-line JET equilibrium code EFIT and it has been found that they provide quite good evaluations of the required quantities, since the differences between their estimates and the EFIT ones are of the order of a few percent. They also provide similar performances in terms of accuracy and computational speed and are quite robust in case of poor quality signals.

Both methods are consequently suitable for reliable real-time control systems in JET.

1. INTRODUCTION
In the last years a remarkable progress have been achieved in demonstrating the feasibility of real-time control of Tokamak plasmas. Particular emphasis on this subject is also a consequence of the increased sophistication of new scenarios, like the advanced Tokamaks with extreme shaping (ITER-like) ones. The complexity of these advanced configurations is making increasing demands on the real-time control systems, which have to be at the same time more complex and more reliable.
In this context, the need for a robust real-time determination of the internal inductance l_i and of the magnetic axis radial position R_{MAG} has emerged in JET. Indeed l_i is a fundamental prerequisite to the calculation of important confinement quantities [1] and is of great help in the control of the magnetic configuration and the current profile [2]. The magnetic axis radial position allows a much faster and reliable assessment of the magnetic topology [3].

To determine the best way to provide these quantities in real-time, two different approaches have been tested. The first consists in the development of specific algorithms, which work out the requested quantities on the basis of the best analytical theory available and with computational methods compatible with constraints for the real-time. The alternative method is a connectionist approach based on specific Neural Networks (NNs), which have been trained with the same inputs as the previous case. In both cases, the best off-line magnetic equilibrium code available, EFIT [4], has been selected as the reference calculation.

The chosen algorithmic approaches and the NNs are based on the determination of the Shafranov Integrals (*SIs*) S_1, S_2 and S_3 [5,6]. These quantities are indeed required: a) they are a prerequisite to the direct calculation of l_i [6] and R_{MAG} (see later); b) being surface integrals of the poloidal magnetic field (see next section for details), they can be computed on a sub-millisecond time scale compatible with the design specifications of the JET real-time control applications.

The paper is organized as follows. A general introduction to the issue of determining the internal inductance and the radial position of the magnetic axis is provided in section two. The main reasons behind the strategic choices made are explained and the theoretical background is shortly presented. The topic of determining the Last Closed Flux Surface (LCFS) is also addressed. The algorithm to evaluate l_i is described in detail in section three; here a brief introduction to NNs is also given, as well as a description of the NNs used in this work and the NN specifically designed to calculate l_i. The results of both methods are then compared with the reference values provided by the EFIT code. Then in section four the R_{MAG} determination is addressed. Finally, section five provides an overview of the relative merits and drawbacks of the two approaches for this kind of application.

2. LAST CLOSED FLUX SURFACE AND SHAFRANOV INTEGRALS

The JET external magnetic measurements are used as an input to the real-time algorithm called XLOC [7]. This code has already been in operation for many years for controlling the plasma shape in JET; it allows the fast determination of the poloidal magnetic flux ψ and consequently the determination of the poloidal magnetic field, external to the plasma column, using the vacuum region approximation. The knowledge of the magnetic field outside of the plasma makes possible the calculation of S_1, S_2 and S_3, integrals of the poloidal field at the plasma boundary. From these quantities a calculation of l_i can then be inferred. The *SIs* can also be used to evaluate R_{MAG}. However l_i and R_{MAG} could not have been obtained without having a fast method to compute in real-time the LCFS necessary to derive the *SIs*, and this has been achieved with an upgrade of XLOC.
The three Shafranov integrals S_1, S_2 and S_3 are defined over the LCFS by [6]:

$$S_1 = \frac{1}{B_{pa}^2 V} \int_S B_p^2 (R\overline{e_R} + Z\overline{e_Z} - R_c \overline{e_R}) \cdot \overline{n} dS \tag{1}$$

$$S_2 = \frac{1}{B_{pa}^2 V} \int_S B_p^2 R_c \overline{e_R} \cdot \overline{n} dS \tag{2}$$

$$S_3 = \frac{1}{B_{pa}^2 V} \int_S B_p^2 Z\overline{e_Z} \cdot \overline{n} dS \tag{3}$$

where $\boldsymbol{B}_p$ is the poloidal magnetic field, S is the plasma surface, R and Z the radial and vertical coordinates ($\boldsymbol{e_R}$ and $\boldsymbol{e_Z}$ the respective vectors), R_c a constant major radius (taken equal to 2.96 m, i.e. the radial coordinate of the vessel centre), V the plasma volume, B_{pa} the poloidal field for normalization[1] and $\boldsymbol{n}$ the vector normal to the plasma surface.
The main difficulty, in calculating these integrals, resides in the evaluation of the LCFS: this quantity can be obtained by mean of the poloidal flux ψ external to the plasma. As already said, in JET the spatial distribution of this quantity is given in real-time by the XLOC code. This code is optimized to match the external magnetic measurements and provides a mapping of the magnetic field. In particular, the poloidal magnetic field in the external region of the plasma is obtained with the following relations:

$$B_R = -\frac{1}{R}\frac{\partial \psi}{\partial Z} \qquad B_Z = \frac{1}{R}\frac{\partial \psi}{\partial R} \tag{4}$$

where B_R and B_Z are the radial and vertical components of the magnetic field.

The determination of the LCFS is then achieved with an upgraded version of XLOC [8], which again satisfies the real-time constraints and can provide the plasma boundary in less than 1 ms (value measured on an 400 MHz Pentium II). As Ψ is a function of R and Z, the procedure mainly consists in tracking the boundary flux value ψ_{LCFS} (provided by XLOC) along one hundred predefined radial segments, called Gaps, whose layout, together with a plasma LCFS, can be seen in fig. 1. The flux has a monotonic trend from inside to outside the plasma: this is a crucial factor that allows the use of the bisection as a fast search method. Indeed the monotonicity guarantees the existence of a unique solution of the expression $\Psi(R, Z) = \Psi_{LCFS}$ along each Gap, and the bisection allows to found this solution with an efficiency of $O(\log_2 N)$ cycles, where N is the number of points of each Gap. Accordingly, the point of each Gap whose flux value is the closest to Ψ_{LCFS} can be considered as belonging to the LCFS.

Having the coordinates of the LCFS and consequently the values of the magnetic field on it, the required *SIs* can be evaluated accurately and rapidly. Fig. 2 shows a typical example of the *SIs* evolution during a discharge in comparison to the EFIT calculation. In table I the performances with respect to EFIT for the whole database[2] are shown. The agreement with the EFIT outputs is satisfactory and therefore these estimates of the Shafranov Integrals are suitable to the evaluation of the internal inductance.

3. DETERMINATION OF THE INTERNAL INDUCTANCE

A) ALGORITHMIC METHOD

The rationale, behind the work devoted to the plasma boundary identification, resides in the fact that, for elongated plasmas, the internal inductance can be expressed in terms of the Shafranov Integrals. If this hypothesis is verified,

l_i is related to these integral quantities by the following expression [6]:

$$l_i = \frac{1}{\alpha - 1}\left[S_1 + S_2\delta - 2S_3\right] \tag{5}$$

where

$$\delta = 1 - \frac{R_t}{R_c}\,. \tag{6}$$

The radial current centroid R_t [1,9] and the parameter α [6] are defined as

$$R_t = \sqrt{2Y_1 R_c + R_c^2} \tag{7}$$

$$\alpha = 2\int_V \left(\overline{B_p} \cdot \overline{e_Z}\right)^2 dV \,/\, \int_V B_p^2 dV \,. \qquad (8)$$

In the previous relation $\boldsymbol{e_Z}$ is the vector of the vertical axis and Y_1 the first Shafranov moment [1,9,10]:

$$Y_1 = \frac{\oint_\Gamma \left\{\left[R - R_c + \frac{1}{2R_c}(R - R_c)^2\right]B_t + \frac{RZ}{R_c}B_n\right\}dl}{\mu_0 I_p} \,. \qquad (9)$$

B_t and B_n are respectively the tangential and normal component of the poloidal magnetic field along the boundary Γ of a plasma cross-section. It is worth noting that both Y_1 and Y_2 (see below) can be determined using the LCFS coordinates and the magnetic field.

The most difficult point in the evaluation of l_i resides in the calculation of α. This volume quantity is sometimes approximated and expressed in terms of the elongation k as [6]:

$$\alpha \cong \frac{2k^2}{k^2 + 1} \,. \qquad (10)$$

Unfortunately relation (10) is not sufficiently accurate for JET applications. Indeed to reduce the errors on l_i below 10% a better evaluation of this quantity had to be devised. To resolve this issue, the calculation of an ideal α_I has been performed, inverting (5), on a reduced database of 21 pulses, using the l_i values provided by EFIT. This ideal α_I has been found to depend mainly on k, on the Shafranov moment Y_2 [10] and on the quantity α_S. The quantities α_S and Y_2 are defined as follows:

$$\alpha_S = \int_S \left(\overline{B_p} \cdot \overline{e_Z}\right)^2 dS \,/\, \int_S B_p^2 dS \qquad (11)$$

$$Y_2 = \frac{\oint_\Gamma \left[f_2 B_t + R g_2 B_n\right]dl}{\mu_0 I_p} \qquad (12)$$

where S is the plasma surface, and

$$f_2 = \left[(R - R_t)\left(1 + \frac{R - R_t}{2R_t}\right)\right]^2 - \left[(Z - Z_t)\left(1 + \frac{R - R_t}{R_t}\right)\right]^2 \qquad (13)$$

and

$$g_2 = \frac{2(R - R_t)(Z - Z_t)}{R_t} + \frac{(R - R_t)^2 (Z - Z_t) - \frac{2(Z - Z_t)^3}{3}}{R_t^2} \,. \qquad (14)$$

It is worth noting that the expression for the Shafranov moment Y_2 is strictly valid for configurations that are symmetric with respect to the plane Z = 0. It turns out that in our case, mainly due to the x-point configurations, its evaluation gives an approximated value, but however sufficient for our purposes. The quantity α_S, in its turn, contains the same integrand as relation (8), but is computed on the boundary surface *S* instead of being evaluated in the entire volume *V*. This parameter results crucial for a good fitting. Indeed it is the only quantity that, in analogy with α, contains ${B_p}^2$, since on the other hand Y_2 is a function of B_p only and k depends merely on the plasma shape.

On the base of the results presented above it has been decided to approximate α with a linear combination of the three aforementioned quantities and of their mixed products:

$$\alpha = c_1\alpha_S + c_2Y_2 + c_3k + c_4\alpha_S Y_2 + c_5\alpha_S k + c_6Y_2k \tag{15}$$

To derive the linear combination coefficients the inversion of the following over-determined matrix equation

$$[\alpha_I] = [X]\cdot[C] \tag{16}$$

has been performed. In (16), [X] is the 6-column matrix containing the parameters on which α depends and [C] is the vector containing the 6 unknown coefficients. The data patterns considered are about 3000 and come from the previously mentioned 21 pulses. For the inversion of the matrix the Singular Value Decomposition method has been chosen. The coefficients determined in this way have then been used to perform the calculation of α in real-time, providing much better results than the approximation (10). In particular, it is worth mentioning that the adopted method allows an optimization of the coefficients that is valid both for the limiter and the x-point phase of the discharge. With the determination of the parameter α previously described, the plasma inductance can now be calculated according to relation (5).

B) NEURAL NETWORKS

The same quantities used in the algorithmic technique previously described, i.e. the *SIs*, k, Y_2, α_S and δ, have also been used as inputs to a specific NN, expressively designed to estimate the plasma internal inductance.

NNs can be considered as non-linear mathematical functions [11] that can provide the determination of a quantity when the expression to be computed is very complicated or even unknown. Indeed they do not need the relationship between input and output to be known, since their computational ability is based on how well they can learn it from the available examples. This means that NNs must be trained to associate the right output to a certain input of the training set, in order to be able to reproduce the right association for those inputs not belonging to the examples. This kind of NNs is the most widely used by the applications, and these networks are known as feedforward supervised NNs.

Topologically they are structured as a Multi-Layer Perceptron, i.e. they consist of a layer of inputs, one or more inner (usually known as hidden) layers, and a layer of outputs. Each layer is made of units: each unit of a layer is connected to all the units of the previous and of the following layer. It can be demonstrated that at least in principle every continuous function can be reproduced by a feedforward NN with a single hidden layer, for a finite range of values of the inputs.

From what stated before, it turns out that the most difficult and time-demanding phase is the one devoted to the training of a NN, since during their actual use NNs can be considered as simple transfer functions. Usually NNs are trained by back-propagating the error of their output with respect to the output supplied by the examples. Several methods have been developed to propagate this error. The Levenverg-Marquardt method is a very fast and robust one and it is well suited to sum-of-squares error function, as in our case.

The database for the training phase consisted in an overall number of 6100 data patterns, of which about 4000 were belonging to the training set and 2000 to the validation set. To check the goodness of the NNs, a test set made of about 1400 patterns has been used. All these patterns belong to the already mentioned database of 54 pulses.

C) COMPARISON OF THE RESULTS OF THE TWO METHODS

The NN structure for the determination of l_i is the following: from subsection 2b it turns out that the NN has seven inputs; instead the number of hidden units has been chosen, after several tests, to be ten; the number of outputs is obviously one.

The evolution of the l_i estimates during a shot is shown in fig. 3. The thin solid curve is the signal computed by the algorithm; the dotted curve is the NN one; the thick solid curve is the result of the off-line EFIT calculation. A statistical comparison between the results of the algorithmic method and the NN approach for the real-time evaluation of l_i is reported in table II. The performances have been computed on the same patterns of the test set, which are patterns neither used for the training of the NN nor for the determination of the α coefficients. These results can be seen, graphically, in fig. 4(a) (algorithm) and 4(b) (NN): on the x-axis the estimates from the algorithm/NN are reported, while on the y-axis there are the ones from EFIT; the more the points are close to the bisectrix, the more the real-time estimates are equal to the off-line ones.

Both techniques provide quite good performances, since the differences with respect to EFIT are normally less than 3%, even if the NN accuracy seems to be on average better than the one of the algorithm. This becomes particularly evident for discharges belonging to the equilibrium classes contained neither in the NN training database, nor in the database used to extract the coefficients for the α calculation.

A test has then been carried out to check the robustness of the two techniques to the noise superimposed to a single input. The magnitude of the noise was +/- 5% with respect to the maximum value of that input. The results are summarized in table III, and are averaged over all the seven inputs. In this case the NN ability of generalize seems to be quite lacking (the MRE worsens of about 40% with respect to the case without superimposed noise). To explain this, it must be considered that the NN has not been trained with noisy data, and so the presence of a noisy input signal becomes crucial when having inputs that are not redundant, as in our case.

4 DETERMINATION OF THE MAGNETIC AXIS RADIAL POSITION

Once the plasma internal inductance has been determined, the Shafranov Integrals allow also calculating the radial position of the magnetic axis. Indeed an estimate of R_{MAG} is given by the following (see [12]):

$$R_{MAG} = R_0 + \frac{a^2}{2R_0}\left(\beta_{MHD} + \frac{l_i}{2}\right)\left(1 - \frac{a}{R_0}\right) + 0.01 \tag{17}$$

(where a is the plasma minor radius, R_0 the plasma major radius and 0.01 is a correction factor normally valid in JET discharges). But since the Shafranov Integrals can be used to estimate the MHD plasma beta β_{MHD} with [5]

$$\beta_{MHD} = \frac{S_1}{2} + \left(1 - \frac{\delta}{2}\right)S_2 - \frac{l_i}{2} \tag{18}$$

it turns out that

$$R_{MAG} = R_0 + \frac{a^2}{2R_0}\left(\frac{S_1}{2} + \left(1 - \frac{\delta}{2}\right)S_2\right)\left(1 - \frac{a}{R_0}\right) + 0.01\,. \tag{19}$$

In this case, it has been possible to implement relation (19) directly without making recourse to specific fitting procedures, as was the case for l_i. Moreover, a and R_0 are quantities that can be easily computed knowing the coordinates of the LCFS.

The evaluation of R_{MAG} has been performed with a dedicated NN as well. The inputs to the NN are the same five quantities appearing in (19), i.e. the two Shafranov Integrals S_1 and S_2, a, R_0 and δ. In this case, after several tests, the number of hidden units has been set to eight.

In fig.5 the two estimates (algorithm and NN — thin solid and dotted curve respectively) of the magnetic axis radial position are compared with the EFIT output (thick solid curve) for a typical discharge. The results of a statistical comparison of the algorithm and of the NN performances is reported in table IV. Also in this case the performances have been computed on the same patterns of the test set. Again, fig. 6 shows graphically the statistical comparison between the real-time signals and the EFIT one. Once more, both approaches give more than acceptable results and the higher flexibility of the NN is also confirmed.

In this case a robustness test has been carried out too. The performances are reported in table V and the same considerations as the l_i case are valid.

5. CONCLUSIONS AND FUTURE DEVELOPMENTS

To summarize, it can be stated that both the algorithmic method and the NN approach give more than acceptable results, satisfying the requirements of JET real-time control system. As far as the time resolution is concerned, the code implementing the algorithmic calculation of l_i and of R_{MAG} provides these quantities in less than 1 ms on an off-line PC, equipped with a 400 MHz Pentium II, with Windows NT as operating system. The NN is even faster since, computationally, can be considered equivalent to a simple transfer function.

From the point of view of the accuracy, both techniques give deviations from EFIT of the order of a few percent in both the limiter and x-point phases of the discharge. These comparable performances, in any case, were somehow expected, since the physical problem to study is well identified and for the required parameters acceptable analytical formulas are available.

If in terms of accuracy and time resolution there does not seem to be great differences between the algorithmic and the connectionist approach, the relative merits of the NNs become clear in terms of adaptability to new equilibrium configuration. This has been interpreted as a higher capacity of the NNs to generalize, compared to strict algorithms which are somehow more rigid in their calculating procedures. It is also worth noting that, in the case that new equilibria or different plasma configurations have to be included, the retraining of the NNs results much easier and less time consuming than the updating of the algorithms.

On the other hand, in term of poor quality measurements, due to high noise or corrupted signals, the performances remain still acceptable, even if the NN ability of generalization seem to weaken. These positive aspects open very good perspectives for the actual use of these methods in JET real-time system. In particular, the code with the algorithmic determination of l_i and R_{MAG} has already been implemented. The l_i computed with the algorithmic method has also already been used, with success, in an experiment session devoted to the real-time control of l_i by mean of the Lower Hybrid Current Drive power. The use of the NNs is also foreseen for the near future.

REFERENCES

[1]. Christiansen J P 1987*Journal of computational physics* **73** 85.

[2]. Joffrin E and Defrasne P 2002 *Review of Scientific Instruments* **73** 2266.

[3]. Zabeo L *et al* 2002 *Plasma Physics and Controlled Fusion* at press.

[4]. O Brien D P *et al* 1992 *Nuclear Fusion* **32** 1351.

[5]. Shafranov V D 1971 *Plasma Physics* **13** 757.

[6]. Lao L L *et al* 1985 *Nuclear Fusion* **25** 1421.

[7]. Milani F 1998 *Disruption prediction at JET* (PhD thesis: University of Aston in Birmingham).

[8]. Barana O *et al* 2002 Real-time determination of global confinement parameters in JET *22nd SOFT conference, Helsinki, September 2002*.

[9]. Brusati M *et al* 1984 *Proceedings of the Second European Workshop on Computational Problems in the Calculation of MHD Equilibria, Wildhaus, Switzerland, September 1983* in *Computer Physics Reports* **1** 345.

[10]. Zakharov L E and Shafranov V D 1973 *Sov. Phys. Tech. Phys* **18** 151.

[11]. Bishop C 1994 *Rev. Sci. Instrum* **65** 1803.

[12]. Shafranov V D 1966 *Reviews of Plasma Physics* **2** 103.

Table I

Shafranov integrals	**MRE (%)**	**MSE**
$\mathbf{S_1}$	3.3	0.001
$\mathbf{S_2}$	4	$1.87e^{-4}$
$\mathbf{S_3}$	2.82	0.0001

Mean relative errors (MRE) and mean squared errors (MSE), with respect to EFIT, of the evaluated Shafranov integrals.

Table II

Internal Inductance	**MRE (%)**	**MSE**
Algorithmic method	2.84	0.0013
Neural Network	1.54	0.00059

Statistical comparison between the algorithmic and the NN estimates of l_i: mean relative errors (MRE) and mean squared errors (MSE) with respect to EFIT.

Table III

Internal Inductance	**MRE (%)**	**MSE**
Algorithmic method	3.71	0.0027
Neural Network	2.14	0.00092

Averaged robustness, to a bad input, of the algorithmic and NN approaches for the l_i calculation: mean relative errors (MRE) and mean squared errors (MSE) with respect to EFIT.

Table IV

Radial Magnetic Axis	**MRE (%)**	**MSE**
Algorithmic method	0.33	1.2e-4
Neural Network	0.073	1e-5

Statistical comparison between the algorithmic and the NN estimates of R_{MAG}: mean relative errors (MRE) and mean squared errors (MSE) with respect to EFIT.

Table V:

Radial Magnetic Axis	MRE (%)	MSE
Algorithmic method	0.66	1e-3
Neural Network	0.22	8.2e-5

Statistical comparison between the algorithmic and the NN estimates of R_{MAG}: mean relative errors (MRE) and mean squared errors (MSE) with respect to EFIT.

Averaged robustness, to a bad input, of the algorithmic and NN approaches for the R_{MAG} calculation: mean relative errors (MRE) and mean squared errors (MSE) with respect to EFIT.

(Footnotes)

[1] $B_{pa} = \sqrt{\dfrac{\mu_0^2 R_c I_p^2}{2V}}$, where I_p is the plasma current and μ_0 is the diamagnetic parameter in the vacuum.

[2] Some things have to be pointed out:

a) the available database consisted of 54 pulses, chosen among the most representative with regard to the different plasma configurations;

b) all the comparisons have been performed by calculating the Mean Relative Error (MRE) and the Mean Squared Error (MSE) of the evaluated quantities with respect to the ones from EFIT;

c) MSE = $\left(\sum_{i=1}^{N} \left\| \dfrac{(S_i^R - S_i^B)}{S_i^R} \right\| \right) / N$ where S^R is the reference off-line signal, S^B is the analogous real-time signal from the algorithmic method or the NN, and N is the total numbers of samples;

d) MSE = $\left(\sum_{i=1}^{N} (S_i^R - S_i^B)^2\right) / N$

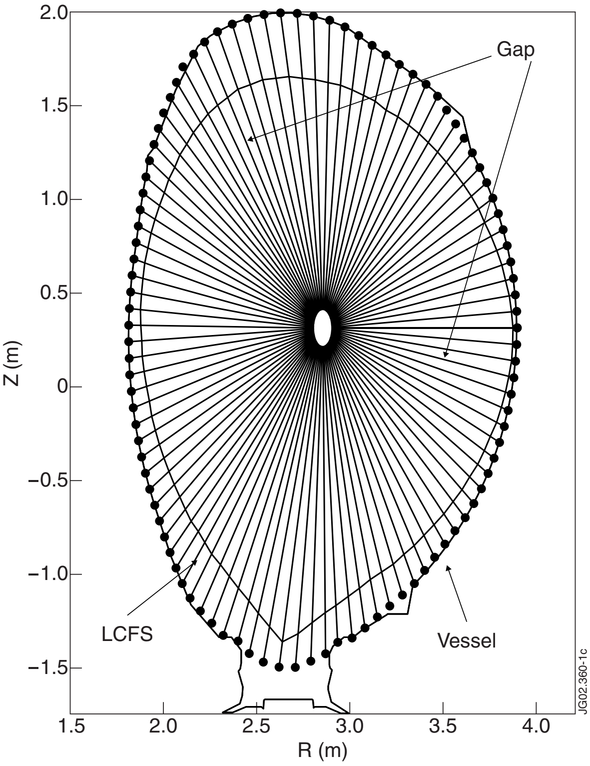

Figure 1: Layout of the one hundred Gaps used in the determination of the Last Closed Flux Surface with an example of it.

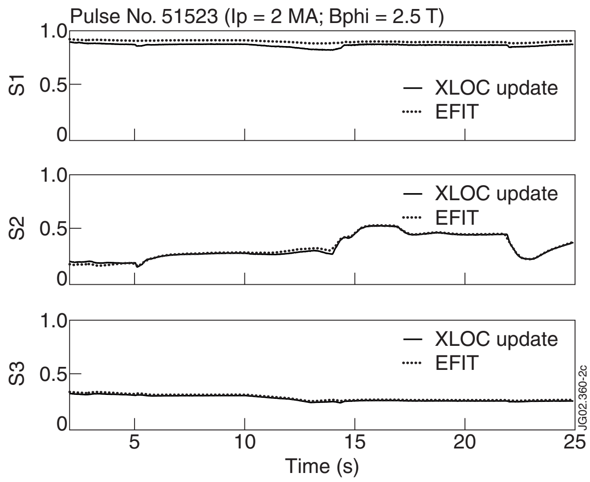

Figure 2: Comparison between the values of S_1, S_2, *and* S_3 *determined thanks to the upgraded version of XLOC (solid line) and by EFIT (dotted line) for Pulse No: 51523; Ip is the plasma current and Bphi is the toroidal magnetic field.*

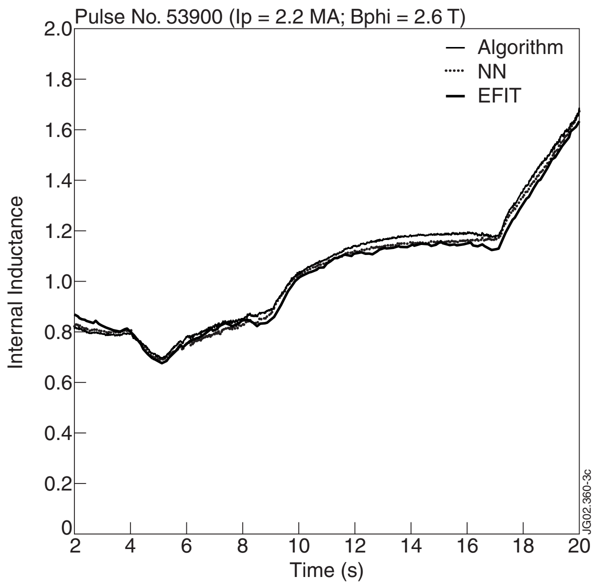

Figure 3: Comparison of the l_i *estimates provided by the algorithmic approach using the* SIs *(thin solid curve), by the NN (dotted curve) and by EFIT (thick solid curve) for Pulse No: 53900; Ip is the plasma current and Bphi is the toroidal magnetic field.*

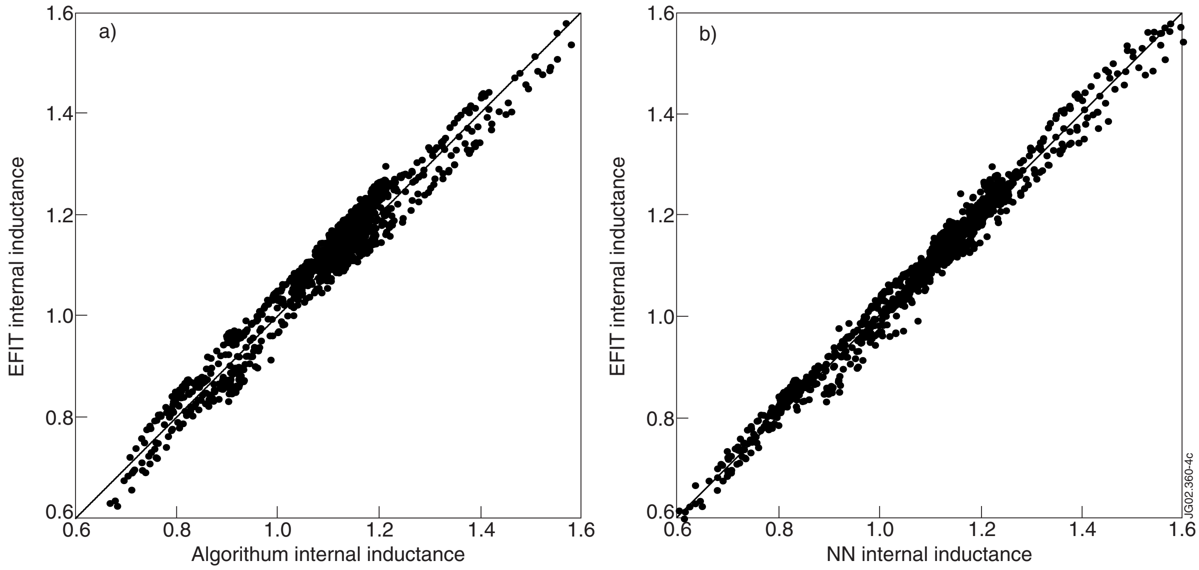

Figure 4: Graphical statistical comparison between the l_i estimates provided by the algorithmic (a) / NN (b) approach and the ones from EFIT.

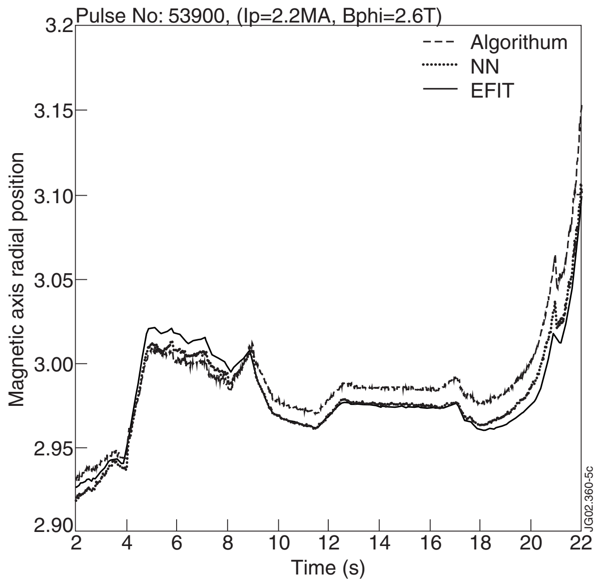

Figure 5: Comparison of the R_{MAG} estimates provided by the algorithmic approach implementing relation (19) (thin solid curve), by the NN (dotted curve) and by EFIT (thick solid curve) for Pulse No: 53900; Ip is the plasma current and Bphi is the toroidal magnetic field.

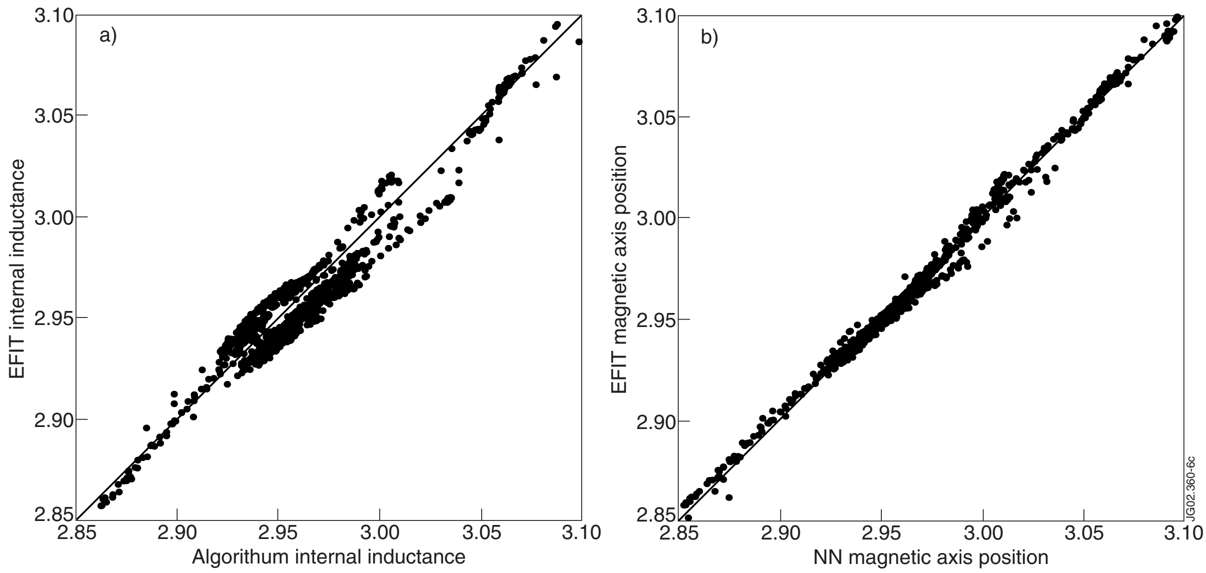

Figure 6: Graphical statistical comparison between the R_{MAG} *estimates provided by the algorithmic (a) / NN (b) approach and the ones from EFIT.*